ELSEVIER

Journal of Molecular Catalysis A: Chemical 111 (1996) 123–133

JOURNAL OF MOLECULAR CATALYSIS A: CHEMICAL

Decomposition of Pt anionic carbonyl complexes in X zeolites. Reactivity of Pt° in the NO + CO reaction. Comparison with the vacuum decomposed $[Pt(NH_3)_4]^{2+}$ complex

J. Nováková [a,*], L. Kubelková [a], P. Hülstede [b], N.I. Jaeger [b], G. Schulz-Ekloff [b]

[a] *J. Heyrovsky Institute of Physical Chemistry, Academy of Sciences of the Czech Republic, Dolejkova 3, 182 23 Prague 8, Czech Republic*
[b] *Institute of Applied and Physical Chemistry, FB2, Bremen University, PF 330440, D-28334 Bremen, Germany*

Received 10 November 1995; accepted 22 April 1996

Abstract

Pt carbonyls were created via reaction of Pt tetraamine complexes in KX and NaX zeolites with CO. The anionic $[Pt_3(CO)_6]_n^{2-}$ Chini complexes formed inside the zeolites were thermally decomposed in vacuum and the residual carbon was combusted under low oxygen pressure followed by hydrogen reduction. Transmission electron micrographs pointed to the formation of Pt° clusters of about 2 nm in size. Carbon deposits, if not removed by oxidation, limited the NO reduction by CO. The decomposition products of anionic carbonyl complexes were compared with those of cationic Pt tetraamine complexes, and the shift of the temperature of ammonia evolution was shown to be one of the proofs of carbonyl formation.

Keywords: Pt carbonyl complexes in KX and NaX; Decomposition; CO + NO reaction

1. Introduction

The preparation of anionic Chini complexes $[Me_3(CO)_6]_n^{2-}$ in zeolitic cavities has been reported in last ten years (Me: Pt, Pd, Rh, Ir [1–10], while their synthesis in homogeneous phase and on basic oxide carriers was successful much earlier [11–17]. The zeolite matrix is very suitable for the formation of short oligomers due to the volume restrictions. Complexes with $n \leq 3$ can be easily embedded in large cavities of faujasites and complexes with higher nuclearity can grow through the zeolite channels, so that even $n = 5$ was found [2–4,10]. A more basic zeolitic matrix leads to the formation of shorter oligomers [1,2,4,10], and thus X zeolites containing heavier alkali cations are more convenient for the preparation of carbonyl complexes of low nuclearity.

If the same nuclearity of metals was retained after decarbonylation of Chini complexes, clusters containing 3–5 atoms would be obtained. However, destruction of the metal frame occurs very readily [18]. Direct measurements of the size of metallic clusters after decarbonylation of Chini complexes both supported or synthesized in zeolites have been scarce: Pt–Pt distances in decomposed Pt Chini complex supported by

* Corresponding author. Tel.: +42-2-66053605; fax: +42-2-8582307; e-mail: povrch@jh-inst.cas.cz.

PII S1381-1169(96)00175-6

MgO examined using EXAFS confirmed the trigonal prismatic structure containing 15 Pt atoms [19], which corresponds with subnanometric dimensions of the Pt particles. High resolution electron microscopy of decarbonylated Rh carbonyls on alumina pointed to the clusters consisting of 6 and 12 (also 18) Rh atoms [20]. TEM and STEM analysis of Pt clusters supported by alumina gave a diameter of 2 nm in agreement with hydrogen chemisorption after reduction at mild conditions (i.e. clusters containing ca. 200 atoms); a higher temperature of decarbonylation (500°C) resulted in formation of particles of 3–10 nm in size [21], i.e. ca. $600–10^4$ atoms. In most cases, only indirect information supporting the presence of highly dispersed metals follows from the shifts of adsorbed CO (e.g. [3,4]) and from the hydrogen and CO adsorption. A high Pt^0 dispersion in NaY after decarbonylation using mild oxidation at 350°C and subsequent reduction at 300°C was reported in [5]; this was based on sorption measurements. IR shifts in adsorbed CO (supported by TEM) pointed to the formation of small Pt clusters in faujasites after decarbonylation at 150°C in 10^5 Pa of CO, while the decomposition in oxygen at ambient temperature lead to the appearance of large Pt crystallites outside the zeolite host [3]. Catalytic activity in structure sensitive reactions also was employed for the estimation of the size of metal particles (e.g. [21]).

The not well defined conditions of the decomposition of carbonyls leading to the formation of small clusters were the reason of the present study concerning the decomposition of Pt Chini complexes in NaX and KX zeolites. The decomposition was checked by mass spectrometric detection of the gases evolved; TPR, adsorption of hydrogen and TEM were employed to characterize the cluster size, and the reactivity of Pt clusters was examined in NO reduction by CO. The same procedures (vacuum decomposition, TPR etc.) were performed with $[Pt(NH_3)_4]^{2+}$ in the same zeolites (this cationic complex was the parent compound used for the synthesis of Chini complexes). Pt clusters obtained by vacuum decomposition of the Pt tetraamine cation in zeolites are known to be heterogeneous in size with diameters between 2 and 4 nm [22–27].

2. Experimental

Preparation and treatment of catalysts. Pt tetraamine complexes were ion exchanged into KX and NaX zeolites (9 and 3 wt% of Pt per undried zeolite, respectively, for details see [28,29]; in only some cases, explicitly specified in text, 3 wt% of Pt in KX was also used). The amine complexes were either directly decomposed in vacuum (similarly as carbonyls, see below), or transformed into Chini complexes in the following way: The samples (20 mg of undried zeolite) were partially dehydrated by evacuation at room temperature for 1 h and allowed to interact with 200 mbar of CO in a 250 ml reservoir at 90°C for 75 h (in some cases only for 24 h). Then the carbonylated sample (further designated PtMeX(Y)/CO) was sealed off from the reservoir and via a breakable connection joined to the apparatus equipped with a Balzers QMG 400 quadrupole mass spectrometer (MS). It was possible to heat the sample in vacuum or in oxygen at low pressures, and also in a stream of oxygen or hydrogen dried by passing through the molecular sieve KA at −78°C. The decomposition of the carbonyls or amines in vacuum was checked using a direct connection to the MS; only an auxiliary pumping system was employed. The samples were first decomposed in vacuum (the highest pressure near the sample was 0.5 Pa) with a heating rate of 2°C/min to 150°C, kept at this temperature for 20 min, and then heated to 400°C (heating rate of 5°C/min). As carbon deposits remained after vacuum decomposition in samples originally containing carbonyls, combustion of these remainders was carried out under 170 Pa of oxygen for several minutes followed by reduction in an hydrogen stream.

^{13}CO exchange for CO in carbonyls and IR + DR UV/VIS spectra of carbonyls. The same amount of ^{13}CO as CO in the carbonyl expected after formation of Chini complex (CO/Pt = 2) was allowed to interact with PtKX/CO (3 wt%) at 90°C. The composition of the gaseous phase was checked using the MS. Diffuse reflectance (DR) UV/VIS spectra were recorded in situ using a Cary 4 spectrometer equipped with a Harrick reaction chamber (for details see Ref. [3]). FTIR spectra of thin zeolite plates (7 mg cm^{-2} in thickness) were also measured in situ using a Nicolet MX–1E spectrometer. Details of these measurements are given in [10].

TPR and TEM examination. The decomposed and reoxidized samples (calcined in oxygen stream at 400°C, 1 h) were reduced by temperature programmed reduction (TPR, for details see Ref. [26,27]). The consumption of hydrogen after the TPR during rapid cooling allowed to compare the Pt surfaces exposed. Transmission electron micrographs [24] were employed for the characterization of the Pt dispersion.

The CO + NO reaction was examined in a static arrangement, in a 'batch' reactor (volume of 400 ml) with a 1:1 mixture of reactants of 200 Pa (total pressure) at 180°C. A negligible amount of the gas mixture was led into the MS using a needle valve. The decrease of pressure during the measurements was due to the reaction stoichiometry (predominant reaction: $2CO + 2NO = 2CO_2 + N_2$). Each reaction was followed by temperature programmed desorption (TPD, 10°C/min, 180–400°C) of surface deposits, the gases released were led directly into the MS.

3. Results

Formation of carbonyls. The formation of carbonyls after the above experimental conditions follows qualitatively from the change in colour (in NaX brick-orange, in KX with 3 wt% also brick-orange and in KX with 9 wt% brick-orange after incomplete carbonylation, green–brown after complete carbonylation). The time plot of the ^{13}CO exchange (gas) for CO in carbonyls (PtKX/CO) at 90°C is given in Fig. 1. As the amount of the parent labelled CO was equal to the amount of CO assumed in Pt carbonyl (CO/Pt ratio = 2), the 1/1 ratio of labelled and unlabelled CO reached in equilibrium supports the formation of the Chini complex. Similar dependencies were found for all carbonyls studied. Further supports of the presence of Chini complexes follow from time resolved UV–VIS and IR measurements [10], where the progress of carbonyl formation is clearly visible.

The FTIR and DR UV/VIS spectra of PtKX/CO and PtNaX/CO are shown in Fig. 2. The bands of $d \rightarrow \pi^*$ transitions found in the UV/VIS spectra at 440, 550 and 350, 690 and 400 nm are typical for $[Pt_3(CO)_6]_n^{2-}$ complexes containing Pt_6, Pt_9 and Pt_{15} clusters, respectively. Formation of the Pt Chini complexes is also confirmed by the bands of stretching vibra-

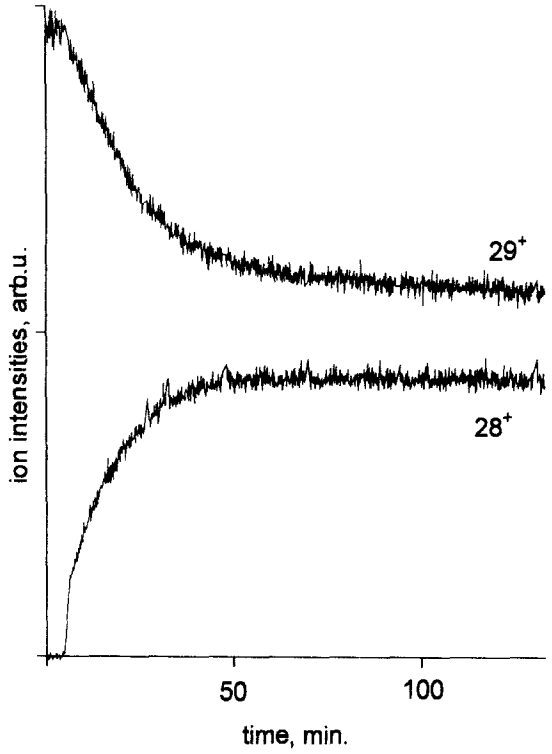

Fig. 1. ^{13}CO exchange for CO in PtKX/CO at 90°C.

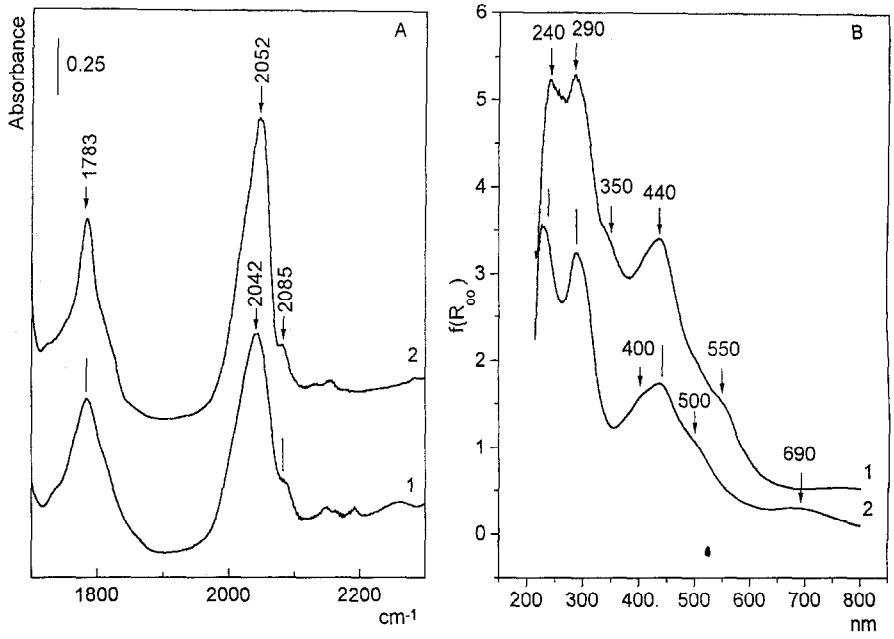

Fig. 2. FTIR (A) and DR UV/VIS (B) spectra of PtKX/CO (1) (3 wt%) and PtNaX/CO (2) carbonylation at 90°C, CO pressure 50 kPa, 24 h (1) and 95 h (2).

tions of CO ligands to Pt atoms in on-top (2042, 2052 cm^{-1}) and bridged bonding (near 1780 cm^{-1}). The shape of the on-top bonds and the maxima frequencies again point to the presence of Pt_6 (2042 cm^{-1}) and Pt_9 (2052 cm^{-1}) carbonyls.

Decomposition in vacuum. The comparison of vacuum decomposition of the anionic Pt carbonyl and cationic Pt tetraammine complex in PtNaX is shown in Fig. 3a and b, respectively. The decomposition up to 150°C (2°C per min, see Section 2) is displayed in the left-hand side of the figure, that with the more rapid heating rate (5°C per min) between 150–400°C is given in the right-hand side. The fractions of the individual compounds were not calculated from these ions due to low accuracy of such calculations in this case, but roughly – considering the ion cross sections of the respective molecules, their fragmentation and properties of our MS – it is possible to relate the bold printed ions ($m/z = X$) to the following compounds: 18^+ to water, ion 16^+ to ammonia (ion intensity should be multiplied by factor 2), 28^+ to

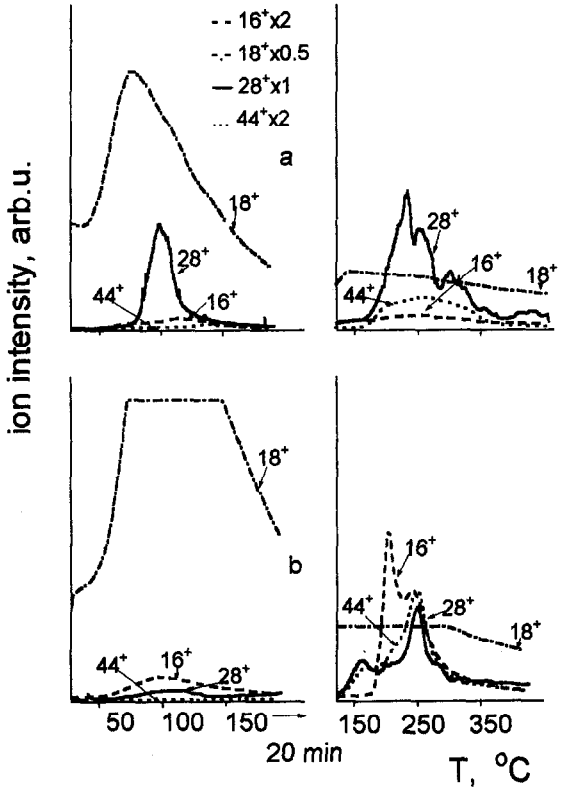

Fig. 3. Vacuum decomposition of PtNaX/CO (a) and $Pt(NH_3)_4$ NaX (b).

CO and nitrogen, 44^+ to CO_2 and 30^+ to NO. It follows from Fig. 3 that ammonia is released together with CO below 150°C from the carbonyl complex (a, left), while almost only water is released in this region from the Pt tetraamine complex (b, left). Above 150°C, CO ($+N_2$) and CO_2 are the only products evolved from the original Chini complex; ammonia is released from the amine complex, being accompanied by $CO + N_2$ in lower fraction than from the carbonyls (for details of the vacuum decomposition of Pt tetraamine ions in faujasites see Refs. [26,27]).

The same dependencies for the vacuum decomposition of carbonyls and $[Pt(NH_3)_4]^{2+}$ in PtKX are shown in Fig. 4: (a) represents the tetraamine complex, (b) the partially carbonylated sample (24 h carbonylation), (c) the completely carbonylated sample. A substantially higher fraction of CO below 150°C appears with the completely carbonylated sample and is accompanied by the evolution of ammonia. In (b), the majority of NH_3 is released above 150°C, which corresponds to the prevailing presence of the amine complex. The maxima of CO evolved from the completely carbonylated Pt (c) appear at lower temperature than for the partially carbonylated sample (b), the first (highest) peak seems to be characteristic for the complete carbonylation. Colours of both (b) and (c) are completely different: (b) is brick-red, similarly as the completely carbonylated less Pt enriched PtNaX, while the completely carbonylated PtKX

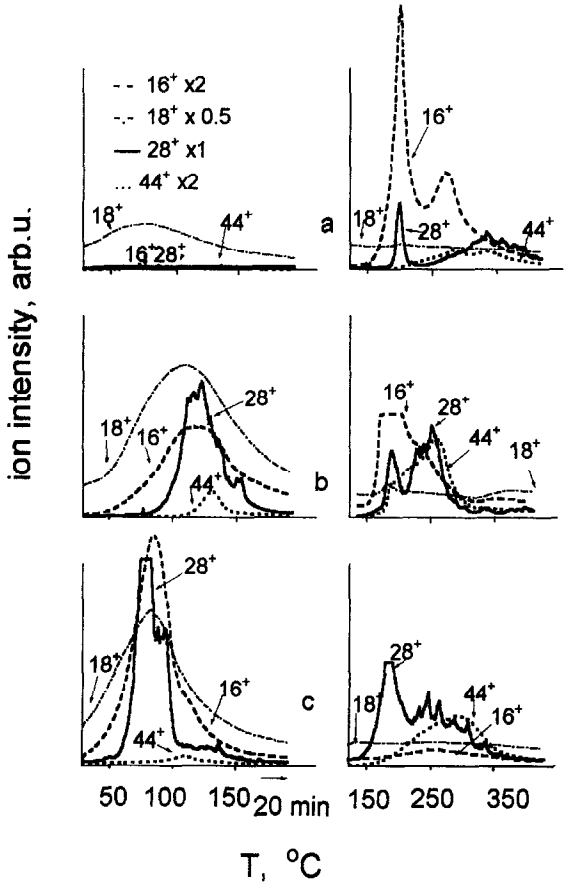

Fig. 4. Vacuum decomposition of $Pt(NH_3)_4KX$ (a), of incompletely carbonylated PtKX/CO (b) and of completely carbonylated PtKX/CO (c).

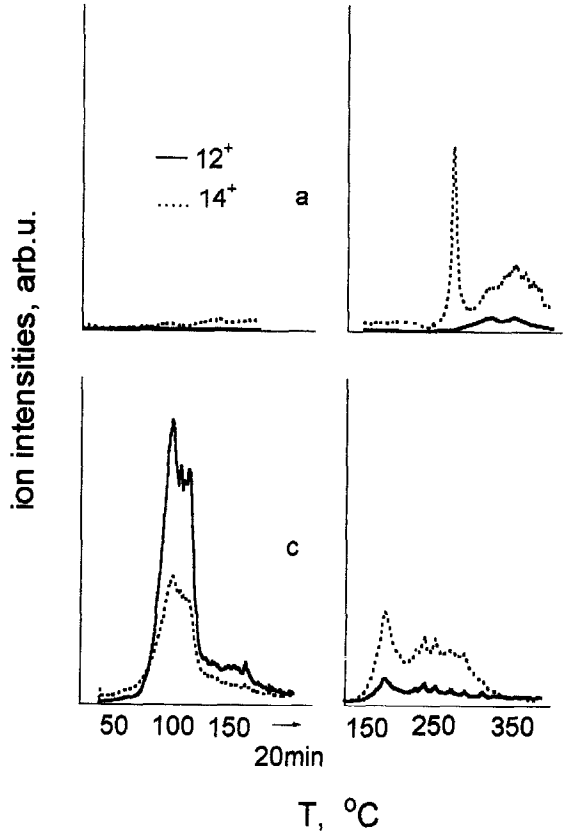

Fig. 5. Separation of CO and N_2 in the ion 28^+ for vacuum decomposition of $Pt(NH_3)_4KX$ (a) and completely carbonylated PtKX/CO (c).

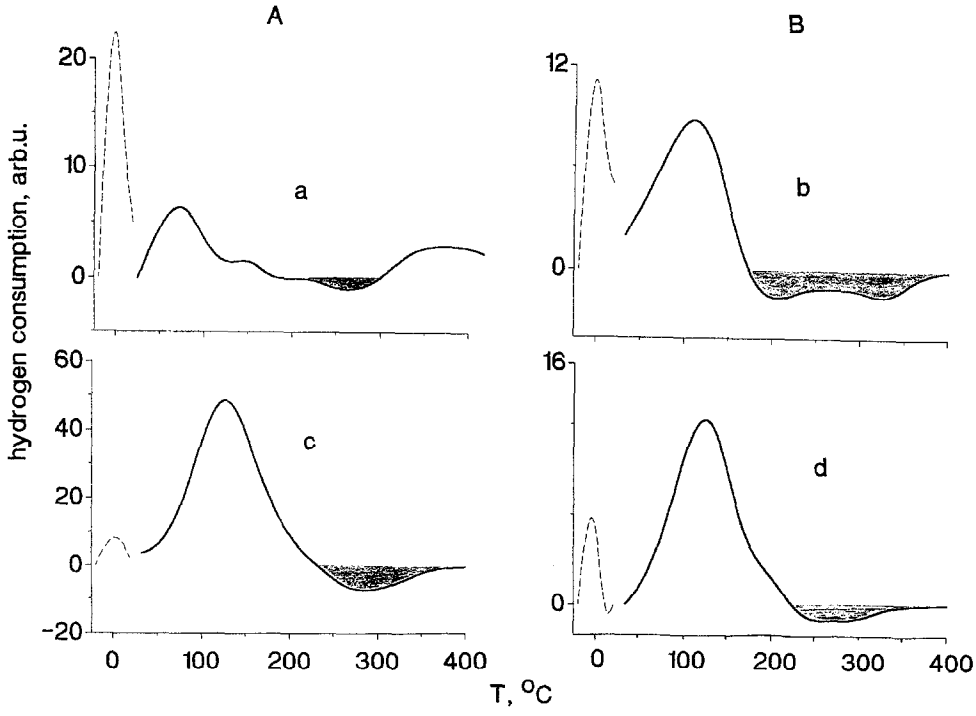

Fig. 6. TPR curves of reoxidized samples. (A) PtKX, (B) PtNaX. (a, b) After the decomposition of tetraamine ions in vacuum, (c, d) after the decarbonylation of Chini complexes in vacuum, – – – (−18)–25°C, ———— 25–400°C.

is brown–greenish. The fragment ions 12^+ and 14^+ can be in some cases employed to separate CO from N_2, as is shown in Fig. 5 (data related to sections a and c of Fig. 4); in our MS the fragment ion $m/z = 12^+$ forms 2% of the molecular peak of CO 28^+, while the fragment ion $m/z = 14^+$ forms 6% of the molecular peak of N_2. It follows from Fig. 5 that nitrogen prevails in the decomposition of the Pt tetraamine ion, only in the highest temperature region CO appears in almost the same amount as N_2 (ion 12^+ must be multiplied by factor 3 to compare the abundance of CO and nitrogen). The Chini complex releases predominantly CO below 150°C (again, the ion 12^+ should be multiplied by factor 3), while above this tem-

Table 1
Adsorption of hydrogen after TPR (H/Pt ratio) and initial CO + NO conversion

Sample	Pt (wt%) [a]	Pretreatment	H/Pt	CO_2/Pt [b]
PtKX (from amine)	9	vac. dec.	0.25	n.d.
		comb.	0.25	6.6
PtKX (from incomplete carbonylation)	9	vac. dec.	0.35	3.9
		comb.	0.35	7.6
PtKX (complete carbonylation)	9	vac. dec.	0.35	1.9
		comb.	0.35	4.1
PtNaX (from carbonyl)	3	vac. dec.	0.33	2.4
		comb.	0.33	8.7

[a] Per undried sample.
[b] % conversion to CO_2 after 10 min, divided by amount of Pt in μmol.

perature both CO and N_2 are present in a comparable ratio. Some CO_2 is released during the vacuum decomposition of both Chini and Pt tetraamine complexes (Fig. 3 and Fig. 4).

TPR and TEM examination. TPR curves of reoxidized (sequence: vacuum decomposition of Pt complexes, reduction, reoxidation) PtKX (A) and PtNaX (B) are depicted in Fig. 6: after the decomposition of Pt tetraamine ions (Fig. 6a and b) and after the decomposition of carbonyls (Fig. 6c and d). Full curves depict the TPR between room temperature and 400°C, dashed curves show the reduction from −18°C to room temperature. The H/Pt ratios, calculated from hydrogen adsorption during rapid cooling after the TPR, are listed in Table 1. The decomposition of the tetraamine complex $[Pt(NH_3)_4]^{2+}$ in vacuum leads to a little lower adsorption than that for decomposed carbonyls. Shadowed areas in the TPR curves correspond to the desorption of hydrogen from metallic Pt created during the reduction. The consumption of hydrogen in TPR and adsorption measurements for NaX is lower than for KX due to 3× lower Pt load in the former case.

TEM micrographs (Fig. 7) show a higher and more homogeneous dispersion of Pt in vacuum decomposed carbonyls (a) than in amine complexes (b). The TEM micrographs were taken from PtKX with 3 wt% of Pt which behaves in the same manner as PtNaX (3 wt% of Pt), as concerns the dispersion of Pt.

CO + NO reaction. The time course of NO reduction by CO at 180°C over PtKX is shown in Fig. 8 for completely carbonylated sample decomposed in vacuum (a), after TPD following this reaction and combustion of surface deposits (b), over decomposed PtKX amine complex in vacuum (c) and after following reduction (d). Ion intensities are recalculated directly to the fractions of reactants and products. The reactant CO and the products N_2, CO_2 and N_2O were separated using ^{13}CO (ions 29^+, 28^+, 45^+ and 44^+, respectively, instead of the same mass/charge ratio 28 for CO and N_2, and 44 for CO_2 and N_2O without labelling). It can be

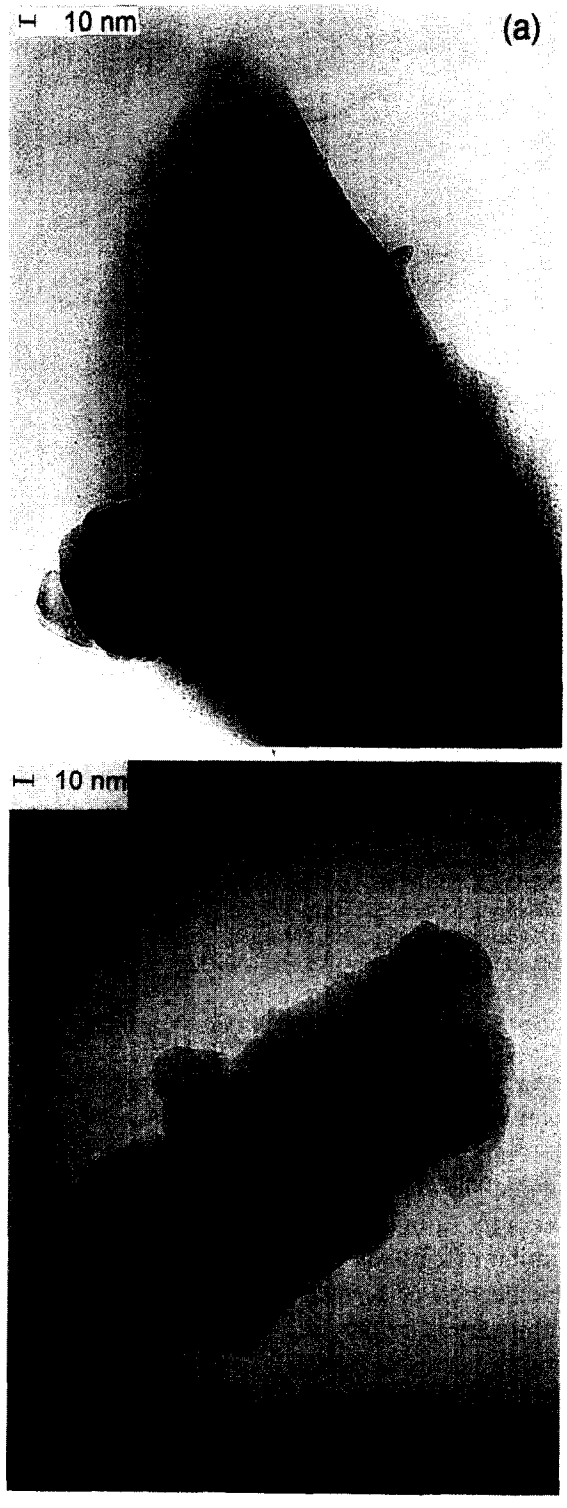

Fig. 7. TEM micrographs of PtKX with 3 wt% of Pt, (a) after the decomposition of Chini complexes in vacuum, (b) after the decomposition of tetraamine ions in vacuum.

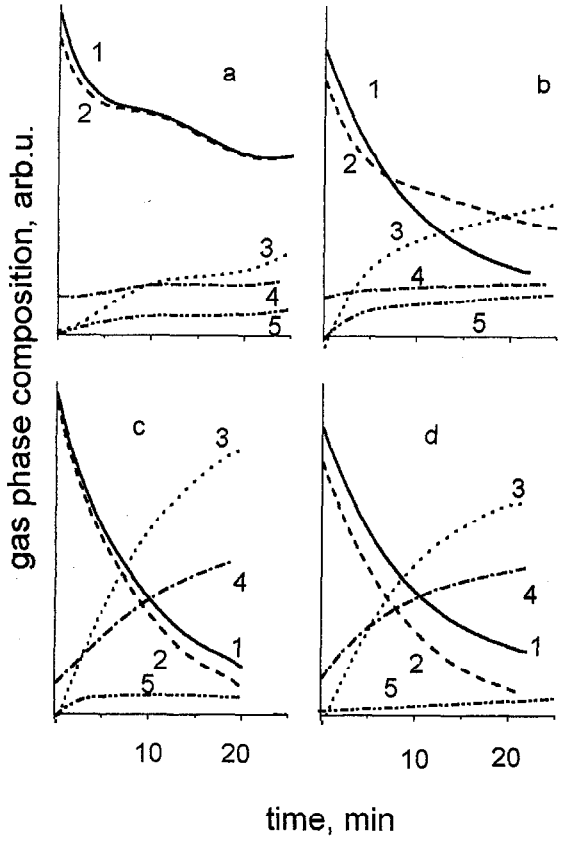

Fig. 8. CO+NO reaction at 180°C over PtKX (decomposed PtKX/CO, after complete carbonylation), and over decomposed $Pt(NH_3)_4KX$. (a) After vacuum decomposition, (b) after TPD and combustion of surface deposit, both originally carbonyls; (c) after vacuum decomposition and combustion, (d) after following reduction – (c) and (d) originally Pt tetraamine ions curves: 1CO, 2NO, $3CO_2$ $4N_2$, $5N_2O$.

seen that: (i) the reaction proceeds more rapidly over decomposed tetraamine complex than over decomposed carbonyl (c versus b), and no substantial effect of reduction following vacuum decomposition of amine appears (d versus c; similar effect was found for carbonyls), (ii) the combustion of surface species after vacuum decomposition of the carbonyl enhances the reaction (b versus a), and (iii) the fraction of N_2O in the gas phase is low, especially in more rapid reactions over decomposed Pt tetraamine complex (curves 5). The other decomposed carbonyls and amines exhibit very similar features. The initial conversion to CO_2 (after 10 min), related to the amount of Pt (in mmol of Pt in the sample weight) is listed in Table 1 for various decomposed carbonyls and amines. It follows, in agreement with Fig. 8, that the combustion of surface species increases the rate at least twice. The decomposed amines exhibit higher activity than decomposed carbonyls, especially if the carbonylation was complete. This difference would be even higher, if the Pt cluster size and conversion per Pt surface exposed were considered (cf. TEM, Fig. 7 – lower dispersion of Pt in decomposed amines than in decomposed carbonyls, and also Pt/H ratios, slightly higher for decomposed carbonyls). The activity of the decomposed PtNaX/CO, related to the amount of Pt, is similar to that of the decarbonylated PtKX/CO.

TPD of surface species formed during the CO + NO reaction over KX before and after combustion of carbon deposit on KX with de-

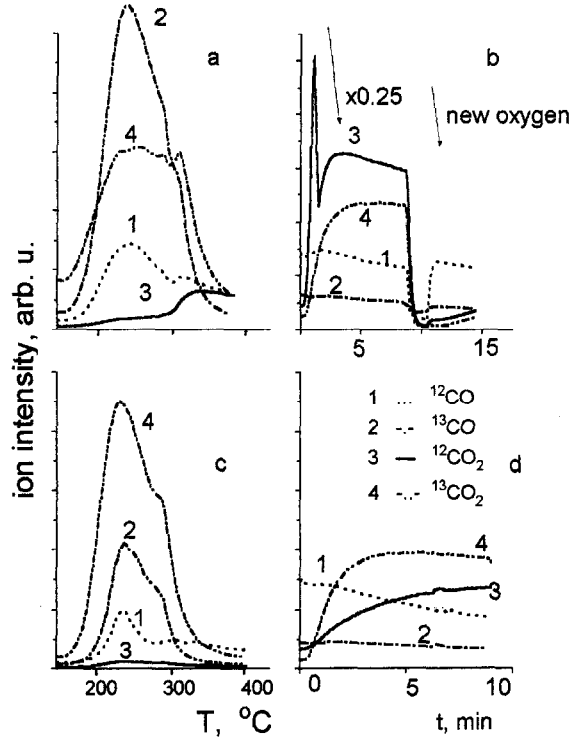

Fig. 9. TPD of surface species after CO+NO reaction (left-hand side), and combustion of remaining surface species after TPD (right hand side). (a) TPD after CO+NO reaction over vacuum decarbonylated PtKX/CO, (b) following combustion at 400°C, (c) TPD after reaction following procedure (b), (d) combustion at 400°C following (c).

composed carbonyl; combustion of the deposit. Temperature programmed desorption (TPD) of CO and CO_2 after the CO + NO reaction is displayed in the left-hand side of Fig. 9 (a) from decarbonylated Pt in KX; the decarbonylation was not followed by the combustion of surface deposit. The right-hand side (b) displays the combustion of carbon deposits after (a). Section (c) shows TPD again after CO + NO reaction, but with the sample after procedure (b), i.e. after combustion of C deposits. Section (d) displays the combustion following TPD (c). It can be seen that the surface deposit is formed predominantly during the decarbonylation, and only from much minor extent during the CO + NO reaction (cf. (a) versus (c), and (b) versus (d)).

4. Discussion

Formation of carbonyls in NaX and KX. The transformation of Pt tetraamine cations into Pt carbonyl anions in our zeolites follows from (i) both DR UV/VIS and FTIR spectra of CO vibrations (Fig. 2), (ii) the marked temperature shift of the release of ammonia to lower temperature in the decomposition of carbonyls compared to amines (Fig. 3 and Fig. 4), (iii) the release of CO from carbonyls (Figs. 3–5), (iv) the CO/Pt ratio = 2 in the ^{13}CO exchange for ^{12}CO of carbonyls (Fig. 1), and (v) the colour of the samples.

Decomposition of anionic and cationic Pt complexes. The decomposition of these two different Pt species proceeds in a different way, as mentioned in the above paragraph. Ammonia is released from carbonyls during their decomposition at temperatures corresponding to the deammoniation of NH_4X zeolites (during the carbonylation Pt amine cations are replaced by NH_4^+), while the amine complexes evolve ammonia at substantially higher temperature. The temperature of the ammonia release can serve as a proof of complete carbonylation: in Fig. 4, section (b), the NH_3 evolution proceeds in both the 'low' and 'high'-temperature region, which points to the incomplete carbonylation. In contrast, no ammonia release is present at higher temperature from completely carbonylated Pt (section (c), Fig. 4).

The decarbonylation temperature of anionic CO complexes in our NaX and KX zeolites agrees with that reported in the literature [5]. The main CO removal proceeds within 80–120°C (Fig. 3 and Fig. 4); if the carbonylation is not complete, it occurs near the higher value (Fig. 4c). These two figures also show that a second, though less intensive, release of CO takes place within 150–350°C. This CO ($+N_2$) release is also observed during the decomposition of the relevant Pt tetraamine complexes. The evolution of CO from the amine complexes is lower than that from the anionic carbonyl complexes and in both cases can be related to the decomposition of surface carbonates, as also CO_2 is removed. The formation of CO_2 during the carbonylation corresponds with the assumed stoichiometry of this reaction [10], so that its release during decarbonylation is not surprising. In [5], the WGS reaction was assumed to result in CO_2 formation. Although it was possible to remove carbon oxides by evacuation at 400°C, some carbon remained in the samples after decarbonylation (in [28] presumably due to CO disproportionation); it was possible to remove it by combustion with oxygen. Even mild oxidation at 250°C removed the carbonaceous species which were also found in [5], and removed in a similar way.

Nitrogen is also released during vacuum decomposition as follows from Fig. 5; its evolution in the decomposition of amine complexes characterizes the Pt autoreduction [22–27]. The amount of N_2 is considerably lower during the decomposition of Chini complexes than during the decomposition of amines (cf. sections (a) and (c) of Fig. 5), which again points to the transformation of amine to carbonyl complex.

Pt° clusters. It follows from the hydrogen adsorption as well from the TEM micrographs that the Pt nuclearity of carbonyls was not retained in the metallic particles in our samples.

Clusters containing 6 and 9 (maximum 15) Pt atoms should be formed in our samples (as n in Pt Chini complexes was 2–3, with NaX also 5 [10]), but the average size observed by TEM is ~ 1.8 nm, i.e. ca. 140 Pt atoms [29]. The cluster size was almost the same, if the decomposition was performed in the oxygen atmosphere (opposite to Ref. [3], which reports on a substantial enlargement of Pt clusters after such treatments), or in CO atmosphere. The size of Pt clusters after the carbonyl decomposition was similar to that observed with decomposed Pt carbonyls prepared on alumina surfaces [21]. Our unsuccessful attempt to prepare fine Pt metallic clusters by decomposition of carbonyls agrees with Ref. [18] where a very easy destruction of the original metallic frame is reported. It seems that the metal nuclearity corresponding to that in carbonyls can be retained only after mild decarbonylation at low temperature, when the metal–support bonding is strong enough, so that metal atoms are not mobile and cannot agglomerate in larger particles. Higher temperature and oxidation of carbon deposits weaken this bond, which leads to the formation of metal particles larger than 1 nm. Detailed description of the decomposition of carbonyls leading to the retainment of the Pt nuclearity without deposits containing carbon, is, unfortunately, still missing.

The decomposition of Pt tetraamine ions in vacuum results in a heterogeneous particle size distribution between 1–4 nm in size, which well agrees with the literature data [22–27]. This dispersion is only a little lower than that obtained by the decomposition of Pt carbonyls.

CO + NO reaction. This reaction has been extensively studied over Pt unsupported as well as supported by oxides (e.g. Ref. [30]). Our preceding papers [26,27] concern the reduction of NO by CO over Pt in X and Y zeolites with various alkali cations, in which Pt° was obtained by the decomposition of Pt tetraamine ions in vacuum. The reaction was accelerated by the increasing positivity, diameter and number of alkali cations.

The a little higher and more homogeneous Pt° dispersion formed in the decomposition of carbonyls results in a lower initial conversion compared to the conversion over vacuum decomposed Pt amines (Fig. 6). Even lesser initial activity was found for finely dispersed Pt after calcination and reduction of Pt amine ions (unpublished results). The effect of metal dispersion on the catalytic activity in structure sensitive reactions is well known and may be the reason of the inverse dependency of the initial activities in NO + CO reaction on the Pt size, as the ability to dissociate NO was found to increase with the increasing Pt particle size [31].

Carbon deposits found after the decomposition of carbonyls substantially retard the reaction, as follows from Fig. 5 and Table 1. This is clearly due to the partial occupation of active sites.

5. Conclusions

It has been found that, under the experimental conditions used, the decomposed Pt Chini complexes in X zeolites do not retain the nuclearity of the preceding carbonyls and Pt atoms agglomerate into 1.8 nm clusters in average.

The decomposition of carbonyls proceeds in vacuum within 80–150°C with simultaneous evolution of ammonia from NH_4^+ ions created during the carbonylation. Ammonia from Pt tetraamine complexes is released at substantially higher temperature, and thus this difference in the temperatures of deammoniation can serve as a support for formation (and extent) of carbonylation.

The decomposition of Pt carbonyls in vacuum leaves carbon deposits on the surface which considerably decrease the CO + NO conversion.

Pt° clusters after the decomposition of carbonyls are a little less active in the CO + NO reaction than the samples obtained by vacuum decomposition of Pt tetraamine ions in the same zeolites, which is assigned to higher Pt dispersion in the former samples.

Acknowledgements

This work was supported by the grants of GA AVCR (440105), GA CR (203/93/1245), DFG (113-111 A2 436 CSR) and JA 346/15-1.

References

[1] G.J. Li, T.Fujimoto, A. Fukuoka and M. Ichikawa, J. Chem Soc. Chem. Commun. (1991) 1337.
[2] G.J. Li, T. Fujimoto, A. Fukuoka and M. Ichikawa, Catal. Lett. 12 (1992) 17.
[3] G. Schulz-Ekloff, R.J. Lipski, N. I. Jaeger, P. Hülstede and L. Kubelková, Catal. Lett. 30 (1995) 65.
[4] A. De Mallmann and D. Barthomeuf, Catal. Lett. 5 (1990) 293.
[5] G.J. Li, T. Fujimoto, A. Fukuoka and M. Ichikawa, in: New Frontiers in Catalysis, Proc. 10th Int. Congr. Catal., ed. I. Guczi et al. (Elsevier Sci. Pub., Amsterdam, 1993) p. 1607.
[6] T. Fujimoto, A. Fukuoka, S. Iiama and M. Ichikawa, J. Phys. Chem. 97 (1993) 279.
[7] L. Dixit, G. Lu and L. Guczi, Zeolites 14 (1994) 588.
[8] H. Bischoff, N.I. Jaeger, G. Schulz-Ekloff and L. Kubelková, J. Mol. Catal. 80 (1993) 95.
[9] A. Yu. Stakheev, E.S. Sphiro, N.I. Jaeger and G. Schulz-Ekloff, Catal. Lett. 34 (1995) 293.
[10] L. Kubelková, J. Vylita, L. Brabec, L. Drozdová, T. Bolom, J. Nováková, G. Schulz-Eckloff and N.I. Jaeger, J. Chem. Soc. Faraday Trans. 92 (1996) 2035.
[11] R.G. Vranka, L.F. Dahl, P. Chini and J. Chatt, J. Am. Chem. Soc. 91 (1969) 1574.
[12] J. Chatt and P. Chini, J. Chem. Soc. (1970) 1538.
[13] J.C. Calabuse, L.F. Dahl, P. Chini, G. Longoni and Martinengo, J. Am. Chem. Soc. 96 (1974) 2614.
[14] M. Ichikawa, J. Chem. Soc. Chem. Commun. (1976) 11.
[15] M. Ichikawa, Chem. Lett. (1976) 335.
[16] G. Longoni and P. Chini, J. Am. Chem. Soc. 98 (1976) 7225.
[17] J. Phillips and J.A. Dumesic, Appl. Catal. 9 (1984) 1.
[18] B.C. Gates, Chem. Rev. 95 (1995) 511.
[19] J.R. Chang, D.C. Koningsberger and B.C. Gates, J. Am. Chem. Soc. 114 (1992) 6460.
[20] S. Iijima and M. Ichikawa, J. Catal. 94 (1985) 313.
[21] B.E. Handy, J.A.Dumesic and S.H. Langer, J. Catal. 126 (1990) 73.
[22] D. Exner, N. Jaeger and G. Schulz-Ekloff, Chem.-Ing.-Tech. 52 (1980) 734.
[23] G. Schulz-Ekloff and N. Jaeger, Catal. Today 3 (1988) 459.
[24] D. Exner, N. Jaeger, A. Kleine and G. Schulz-Ekloff, J. Chem. Soc. Fraday Trans. I 84 (1988) 4097.
[25] N.I. Jaeger, A.L. Jourdan and G. Schulz-Ekloff, J. Chem. Soc. Faraday Trans. 87 (1991) 1251.
[26] J. Nováková, L. Kubelková, L. Brabec, Z. Bastl, N. Jaeger and G. Schulz-Ekloff, Zeolites 16 (1996) 173.
[27] J. Nováková, L. Brabec and L. Kubelková, Collect. Czech Chem. Commun. 60 (1995) 428.
[28] H.H. Lamb, Catal. Today 18 (1993) 3.
[29] G.C. Bond, Surf. Sci. 156 (1985) 966; Chem. Soc. Rev. 20 (1991) 441.
[30] K. Taylor, Catal. Rev. Sci. Eng. 35 (1993) 457.
[31] E.J. Altman and R.J. Gorte, J. Phys. Chem. 93 (1989) 1993.